radicals to be 0.53 and 0.97 eV, respectively.[23] The excellent agreement of these values with the experimental electron affinities indicates the potential of the method used by these workers for determining the electron affinities of π radicals.

Conclusions

Photodetachment cross section experiments have been shown to be a sensitive method for measuring the electronic spectra of gas phase negative ions. The positions of $\pi \rightarrow \pi^*$ transitions in some polyene anions are found systematically to occur at longer wavelengths than those for neutral molecules of comparable conjugation. This observation provides evidence that π orbitals in delocalized negative ions are significantly more diffuse than those in neutrals. Finally the experimental electron affinities of polyene radicals are shown to be linearly correlated with both the HMO delocalization energies in the anions and the HOMO energies from PPP calculations on the anions. These correlations may provide a useful method for estimating the electron affinities of other polyene radicals.

References and Notes

(1) For example, see B. Bockrath and L. M. Dorfman, *J. Am. Chem. Soc.*, **96**, 5708 (1974); A. Streitwieser, Jr., and J. I. Brauman, *ibid.*, **85**, 2633 (1963).
(2) See E. T. Kaiser and L. Kevan, Ed., "Radical Ions", Wiley-Interscience, New York, 1968.
(3) (a) D. Spence, *J. Chem. Phys.*, **66**, 669 (1977); (b) P. D. Burrow and K. D. Jordan, *Chem. Phys. Lett.*, **36**, 594 (1975); (c) K. D. Jordan, J. A. Michejda, and P. D. Burrow, *ibid.*, **42**, 227 (1976).
(4) (a) R. N. Compton, L. G. Christophorou, G. S. Hurst, and P. W. Reinhardt, *J. Chem. Phys.*, **45**, 4634 (1966); (b) R. N. Compton, L. G. Christophorou, and R. H. Huebner, *Phys. Lett.*, **23**, 656 (1966); (c) W. T. Naff, R. N. Compton, and C. D. Cooper, *J. Chem. Phys.*, **57**, 1305 (1972); (d) C. D. Cooper and R. N. Compton, *ibid.*, **59**, 3550 (1973); (e) *ibid.*, **60**, 2424 (1974); (f) J. A. Stockdale, F. T. Davis, R. N. Compton, and C. E. Klots, *ibid.*, **60**, 4279 (1974); (g) C. D. Cooper, W. T. Naff, and R. N. Compton, *ibid.*, **63**, 2752 (1975).
(5) U. Fano, *Phys. Rev.*, **124**, 1866 (1961).
(6) G. J. Shulz, *Phys. Rev.*, **125**, 229 (1962); A. Herzenberg and F. Mandl, *Proc. R. Soc. London, Ser. A*, **270**, 48 (1962).
(7) J. H. Richardson, L. M. Stephenson, and J. I. Brauman, *J. Chem. Phys.*, **62**, 1581 (1975); *J. Am. Chem. Soc.*, **97**, 2967 (1975).
(8) A. H. Zimmerman, K. J. Reed, and J. I. Brauman, *J. Am. Chem. Soc.*, **99**, 7203 (1977); A. H. Zimmerman and J. I. Brauman, *J. Chem. Phys.*, **66**, 5823 (1977).
(9) This is probably not the lowest electronic transition in neutral polyenes. See B. S. Hudson and B. Kohler, *Annu. Rev. Phys. Chem.*, **25**, 437 (1974). However it is certainly the lowest transition which has sufficient optical intensity to be easily observed in the spectrum. Because correlation effects are likely to be less important in the relatively diffuse anion, this may also be the lowest energy transition as well.
(10) C_{2v} symmetry is assumed for the polyene anions.
(11) K. C. Smyth and J. I. Brauman, *J. Chem. Phys.*, **56**, 1132 (1972).
(12) A. H. Zimmerman and J. I. Brauman, *J. Am. Chem. Soc.*, **99**, 3565 (1977).
(13) For example the lowest optically allowed $\pi \rightarrow \pi^*$ transitions in ethylene, butadiene, hexatriene, and octatetraene occur at 162.5, 217.0, 251, and 304 nm, respectively; see A. Streitwieser, Jr., "Molecular Orbital Theory for Organic Chemists", Wiley, New York, N.Y., 1961, p 208.
(14) For examples, see C. J. Roothaan and A. W. Weiss, *Rev. Mod. Phys.*, **32**, 194 (1960); E. Clementi, A. D. McLean, D. L. Ramondi, and M. Yoshimine, *Phys. Rev.*, **133**, 1274 (1964); P. E. Cade, *J. Chem. Phys.*, **47**, 2390 (1967); K. M. Griffing and J. Simons, *ibid.*, **62**, 535 (1975); E. Andersen and J. Simons, *ibid.*, **65**, 5393 (1976).
(15) H. Kuhn, *J. Chem. Phys.*, **17**, 1198 (1949).
(16) (a) R. D. Pariser and R. G. Parr, *J. Chem. Phys.*, **21**, 466, 767 (1953). (b) The off-diagonal electron–electron repulsion integrals were calculated according to N. Mataga and K. Nishimoto. *Z. Phys. Chem. (Frankfurt am Main)*, **13**, 140 (1957).
(17) P. Hochmann, R. Zahradnik, and V. Kvasnicka, *Collect. Czech. Chem. Commun.*, **33**, 3478 (1968).
(18) Configuration mixing of all singly excited configurations does not affect the predicted transitions significantly.
(19) (a) The delocalization energies for allyl and pentadienyl anions are from C. A. Coulson and A. Streitwiesser, Jr., "Dictionary of Pi Electron Calculations", Pergamon Press, New York, N.Y., 1965. (b) The delocalization energy for heptatrienyl anion is from A. Streitwieser, Jr., and J. I. Brauman, "Supplemental Tables of Molecular Orbital Calculations", Vol. 1, Pergamon Press, New York, N.Y., 1965, p 12.
(20) D. S. Marynick and D. A. Dixon, *Proc. Natl. Acad. Sci. U.S.A.*, **74**, 410 (1977).
(21) J. E. William, Jr., and A. Streitwieser, Jr., *J. Am. Chem. Soc.*, **97**, 2634 (1975).
(22) T. Koopmans, *Physica*, **1**, 104 (1934).
(23) J. R. Hoyland and L. Goodman, *J. Chem. Phys.*, **36**, 21 (1962).

Photoelectron Spectroscopy of Carbonyls. Lone-Pair Interactions in α-, β-, γ-, and δ-Dicarbonyls

D. Dougherty, P. Brint, and S. P. McGlynn*

Contribution from the Choppin Chemical Laboratories, The Louisiana State University, Baton Rouge, Louisiana 70803. Received February 13, 1978

Abstract: The ionization of the nonbonding electrons, n_+ and n_-, of 73 dicarbonyls (38 α-, 24 β-, 8 γ-, and 3 δ-) have been surveyed experimentally (ultraviolet photoelectron spectroscopy) and computationally (CNDO/s and CNDO/2). Apart from certain readily rationalized exceptions, it is shown that the energy split of the n_+/n_- ionization events is primarily determined by the separation of the two carbonyl groups; that the splitting mechanism involves through-bond interaction with skeletal σ orbitals; and that the Franck–Condon band shapes of $I(n_+)$ and $I(n_-)$ are determined by the nature of the intermixed skeletal σ orbitals. A simple algorithm for $I(n_+)/I(n_-)$ splittings and band shapes is presented.

Introduction

Much work has been invested[1-21] in the ultraviolet photoelectron spectroscopy (UPS) of carbonyl compounds in order to identify the mechanism by which carbonyl groups interact among themselves and with other functional groups. However, many of the UPS assignments are unsatisfactory since they are largely based on the isomorphism between quantum chemical and UPS data sets implied by Koopman's theorem.[22]

A "simple dicarbonyl compound" is one which contains neither heteroatoms (other than two oxygens) nor carbon–carbon unsaturation. The two highest occupied MOs of simple dicarbonyls consist[1,2,12] predominantly of linear combinations
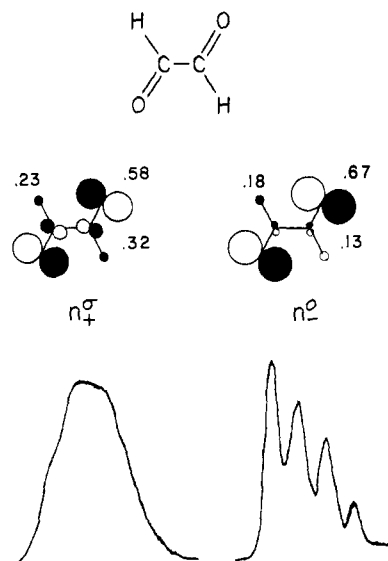
Figure 1. MO diagram of $n_+{}^\sigma$ and $n_-{}^0$ for *trans*-glyoxal. The UPS ionization bands[25] are also schematized. Geometric parameters used in the CNDO/s calculation follow: all bond angles were 120°; the C–C bond length was 1.53 Å; the C=O bond length was 1.22 Å; and the C–H bond length was 1.00 Å.

of the two oxygen nonbonding $2p\sigma$ atomic orbitals, n_1 and n_2. For symmetrical dicarbonyls (i.e., those for which the carbonyl groups are interchanged by some symmetry operation), the two symmetry-adapted, semilocalized functions[1,2] are

$$n_+ = \frac{1}{\sqrt{2}}(n_1 + n_2) \quad \text{and} \quad n_- = \frac{1}{\sqrt{2}}(n_1 - n_2)$$

where the subscripts $+/-$ refer to phasing. The n_+/n_- functions are degenerate in zeroth order.

For nonsymmetrical dicarbonyls, the two semilocalized MOs are

$$n_+ = an_1 + bn_2 \quad \text{and} \quad n_- = bn_1 - an_2$$

where, in the absence of overlap of n_1 and n_2, $b = \sqrt{1 - a^2}$. These functions are nondegenerate in zeroth order.

Purpose of Work

Our aim is to generate criteria for the assignment of the n_+/n_- MOs. Consequently, UPS data are collected for a large number of dicarbonyls. Pertinent assignment criteria are thought to lie in the following considerations: (a) the nature of the interactions which lift the n_+/n_- zero-order degeneracy; (b) the magnitude of the n_+/n_- splitting as a function of the separation of the two carbonyl centers; (c) the n_+/n_- energetic order which results from the splitting; (d) the Franck–Condon shapes of the n_+/n_- ionization bands.

The interactions of item (a) are satisfactorily categorized[1,2,4] in terms of the heuristic concept of "through-bond" interactions.[3] Hence, we will confine ourselves to considerations of items (b), (c), and (d).

The n_+/n_- splitting, which is denoted Δn, is experimentally determinable by UPS. The average value of Δn, $\overline{\Delta n} \equiv |I(n_+) - I(n_-)|$, for a given set of dicarbonyls (i.e., the $\{\alpha$-$\}$, $\{\beta$-$\}$, $\{\gamma$-$\}$, and $\{\delta$-$\}$ sets) is found to be a distinguishing characteristic of the set in that $\overline{\Delta n} \simeq \Delta n$ for most of the members of any one set. Molecules for which $\overline{\Delta n} \neq \Delta n$ do exist, but they are always exceptional in some particularly obvious way.

The n_+/n_- energetic order is usually obtained by MO computations. One attempt[23] at greater generality exists. This study concluded that the MO order should be $n_+ > n_-$ (i.e., $I(n_-) > I(n_+)$) for any through-bond interaction over an odd

number of intervening bonds. We agree with this conclusion, but only when the carbonyl groups are noncoaxial.

The removal of the n_+/n_- degeneracy is accomplished, on a theoretical level, by through-bond mixing with other skeletal σ orbitals. Since these σ orbitals are more tightly bound than the n orbitals, destabilization of the n MOs occurs. Therefore, the more thoroughly mixed n orbital is of higher energy (i.e., less tightly bound) than the less skeletally mixed n orbital.

Ionization of an electron from the more skeletally delocalized n orbital should yield a cation geometry different from that of the neutral ground state. The adiabatic and vertical transitions for such an ionization should be different and the resulting band shape ought to be broad and Gaussian. The removal of an electron from a skeletally nondelocalized n orbital should produce little or no geometry change. The adiabatic and vertical events for such an ionization should coincide. If only approximately coincident, the intensity should drop less sharply to higher energies, generating a band shape which we refer to as "blue degraded". For somewhat obvious reasons,[12] the ionization event of Gaussian band shape is denoted $I(n^\sigma)$ and the blue-degraded event is denoted $I(n^0)$.

Experimental Section

The He I photoelectron spectra were obtained on a Perkin-Elmer PS-18 photoelectron spectrometer which was equipped with a heated sample probe for vaporizing solids. The resolution prior to each run was 20–25 meV. Spectra were calibrated with the ^2P lines of Xe and Ar. Sample temperatures during each run were maintained constant to within ±2 °C. All compounds were purified by vacuum sublimation. Quantum chemical calculations were performed using QCPE 141-CNDO/2 and QCPE 174-CNDO/s-CI.

The Interaction Model

The two semilocalized linear combinations n_+ and n_- are assumed to be degenerate in zero order. The through-space[3] interaction of the individual lone pair AOs on oxygen, n_1 and n_2, is neglected since it is very small.[1,4] Through-bond interaction, therefore, is the principal means of removing the degeneracy. Interaction is supposed to occur between the n_+/n_- MOs and the set of molecular skeletal orbitals $\{\chi_j\}$. This view facilitates a simple representation:

(1) The interacting n_I, where $I = +$ or $-$, and χ_j orbitals must transform identically in the molecular point group.

(2) The magnitude of the n_I/χ_j interaction is inversely proportional to the zero-order energy separation of n_I and χ_j. This energy denominator criterion justifies exclusion of interactions with the virtual orbital set (which, because of its dominant σ^* nature, is of very high energy).

(3) The magnitude of interaction is proportional to the n_I/χ_j interaction matrix element and, hence, to overlap. Thus, the extent of interaction is very sensitive to the amplitude of χ_j in the vicinity of the carbonyl groups.

α-**Dicarbonyls.** α-Dicarbonyls exhibit the largest interactions. The magnitude of the interaction is independent of the dihedral angle between the carbonyl units.[1,4]

Molecular orbital diagrams (CNDO/s) for *trans*-glyoxal are given in Figure 1. They illustrate the correlation between the qualitative interaction model and the computational results for α-dicarbonyls generally. A comparison of UPS band shapes with MO coefficients (see Figure 1) exemplifies the Franck–Condon considerations.

Criteria 1–3 suggest that σ bonds with significant electron density between and/or contiguous to the carbonyls are the only ones which interact strongly with the n MOs. Furthermore, symmetry considerations suggest a greater sensitivity of the n_+ MO. Hence, we use the labeling $n_+{}^\sigma$, where the superscript σ implies that the $I(n_+{}^\sigma)$ event should possess a Gaussian band shape. The less interacted orbital is denoted $n_-{}^0$ and is expected to exhibit a blue-degraded $I(n_-{}^0)$ band shape. Therefore, the MO order is $n_+{}^\sigma > n_-{}^0$ and the band shape
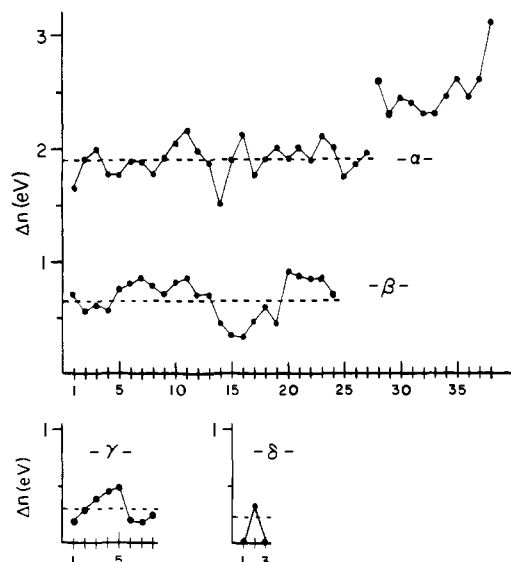
Figure 2. Diagrammatic presentation of Δn for the dicarbonyls of Table I. The numbering index on the abscissa corresponds to the compound number in Table I. The dashed line is the mean of Δn, $\overline{\Delta n}$, from Table II.

Figure 3. MO diagrams for the $n_-{}^\sigma$ and $n_+{}^0$ MOs of 1,3-propanedial. The geometry used in the CNDO/s calculation follows: trigonal carbon angles were 120° while the bond angles about a tetrahedral carbon were 109.5°. The C-C bond length was 1.54 Å, C=O was 1.22 Å, C-H was 1.00 Å on carbons 1 and 3, while C-H was 1.08 Å on carbon 2.

characteristics are Gaussian and blue degraded, respectively.

These comments on UPS band shapes should apply generally. Thus, biacetyl,[9] oxamide,[10] and pyruvamide[9] have $n_+{}^\sigma$ and $n_-{}^0$ band shapes similar to glyoxal. In larger molecules, the mixing of n_+ and n_- with the greater number of skeletal MOs which exists in such molecules produces a loss of structure in $I(n_-{}^0)$, and both $I(n_-{}^0)$ and $I(n_+{}^0)$ exhibit structureless band contours. The $I(n_-{}^0)$ band, however, usually remains sharper than $I(n_+{}^\sigma)$.

The vertical ionization energies for the n MOs of 38 α-dicarbonyls are listed in Table IA. The molecules listed are of quite diverse natures. Although $I(n_+)$ and $I(n_-)$ vary widely, Δn is relatively constant. In fact, for the first 27 compounds, it is found that $\overline{\Delta n}$ = 1.9 ± 0.15 eV (mean and standard deviation). This constancy is emphasized in the plot of Figure 2.

The last 11 molecules of Table IA are of particular interest since they exhibit substantially larger values for Δn.

The abnormally large splitting in tetrafluoro-1,2-cyclobutanedione must be attributed to ring perfluorination because Δn for 1,2-cyclobutanedione is normal. Perfluorination, as evidenced by the perfluoro effect,[24] is known to produce unusual behavior.

A very definitive, special case occurs in the bicyclo[2.2.1]-5-ene-2,3-dione compounds[18,21] (compounds **30–36**, Table IA). The 5-ene moiety is sterically forced to interact, in a through-bond manner, with n_+. Thus, in bicyclo[2.2.1]hept-2,3-dione, in which the 5-ene moiety is absent, Δn behaves normally.

Geometry considerations suggest the existence of through-bond interaction of n_+ with the 7-oxa lone pair in compound **29**, and with the cyclopropyl Walsh orbitals in compounds **37** and **33** of Table IA.

Thus, the large values of Δn for the last ten compounds of Table IA are due to an additional through-bond (or hyperconjugative) interaction which adds onto the "pure" α-dicarbonyl splitting typical, say, of glyoxal. These interactions manifest themselves computationally as a large degree of mixing between the semilocalized n_+ or n_- orbitals and the (usually) localized or semilocalized hyperconjugating orbital of the functional group. In a way, then, the labels $n_{+/-}$ are misleading since they imply a degree of localization which is too extreme.
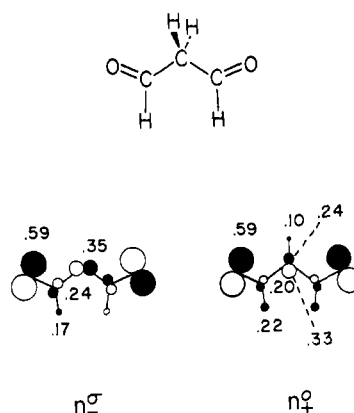
Differences are also observed between the vibrational frequencies associated with the $I(n_+)$ and $I(n_-)$ bands.

The $n_+{}^\sigma$ band, being associated with a considerable alteration of molecular structure, seldom shows vibrational structure. When it does exhibit such structure, it is usually ill defined and of low frequency. For example, in entries **27, 30, 31**, and **36** of Table IA, progressions occur in an interval of ~600 cm^{-1}. Entry **9**, oxamide, exhibits an interval of 440 cm^{-1} and, quite uniquely, a high-energy 1620 cm^{-1} mode.

The vibrational activity in the $n_-{}^0$ band is often quite discrete and is usually of higher energy: entry 1, 1620 cm^{-1}; entry 2, 1510 cm^{-1}; entry 5, 1482 cm^{-1}; entry 9, 1510 cm^{-1}; entry 13, 1530 cm^{-1}; entry 36, 1320 cm^{-1}; etc. It has been supposed[14] that this active mode is a carbonyl stretching vibration.

β-Dicarbonyls. The through-bond interactions in β-dicarbonyls are mediated by two intervening σ bonds. The n MO eigenvectors are schematized in Figure 3 for 1,3-propanedial, the smallest β-dicarbonyl. The calculations of Houk et al.[5] indicate that $n_- > n_+$ (except for the special cases of 1,3-cyclobutanedione and tetramethyl-1,3-cyclobutanedione). These results, when added to our own computational investigations, allow us to impute qualitative generality for the discussion which we base on Figure 3.

The equality of the LCAO MO coefficients for n_+ and n_- suggests that considerable mixing with the skeletal σ orbitals occurs for both nonbonding orbitals in the β-dicarbonyls. It is observed that the σ bonds intervening between the two carbonyl groups overlap more effectively with n_- than with n_+. Consequently, criterion (3), overlap, appears to be largely responsible for the splitting of the n MOs of β-dicarbonyls.

Table IB lists the vertical ionization energies and Δn values for β-dicarbonyls. The behavior of Δn is shown in Figure 2. Acyclic molecules appear first and are followed, in order, by five-membered ring cyclic compounds, six-membered ring cyclic compounds, and 2,2,4,4-tetramethyl-1,3-cyclobutanedione (TMCBD). Several observations are appropriate.

(1) $\overline{\Delta n}$ is considerably smaller for β- than for α-dicarbonyls.

(2) The values of Δn for the unsymmetrical formylurea[15] and acetylurea[15] are slightly larger than those for the simple symmetrical acyclic dicarbonyls.

(3) The value of $\overline{\Delta n}$ for the five-membered-ring cyclic molecules is 0.8 ± 0.1 eV and the values of Δn are quite constant. This constancy may reflect the rigid nature of these systems, or it may be an artifact of a limited data set.

(4) Values of Δn for the symmetrical six-membered ring cyclic molecules (numbers **14–19**, Table IB) are generally

Table I. Vertical Ionization Energies (eV) of the Nonbonding Electrons of Some Dicarbonyls[f]

no. index	compd	$I(n_+)$	$I(n_-)$	Δn
	A. α-Dicarbonyls			
1	HCOCOH[a]	10.52	12.19	1.67
2	CH₃COCOCH₃[b]	9.55	11.46	1.91
3	CH₃COCOOH[b]	10.42	12.42	2.00
4	CH₃COCOOCH₃[b]	9.88	11.66	1.78
5	CH₃COCONH₂[b]	9.71	11.48	1.77
6	HOCOCONH₂[c]	10.51	12.40	1.89
7	C₂H₃OCOCONH₂[d]	9.85	11.73	1.88
8	C₂H₃OCOCON(CH₃)₂[d]	9.31	11.09	1.78
9	H₂NCOCOHN₂[c]	9.80	11.72	1.92
10	HOCOCOOH[c]	11.20	13.25	2.05
11	ClCOCOCl[d]	11.26	13.42	2.16
12	C₂H₅OCOCOCl[d]	10.77	12.76	1.99
13	(CH₃)HNCOCONH(CH₃)[e]	9.33	11.20	1.87
14	bicyclo[2.2.2]octane-2,3-dione[f]	9.0	10.5	1.5
15	bicyclo[2.2.2]oct-5-ene-2,3-dione[f]	8.9	10.8	1.9
16	1,2-cyclobutanedione[g]	9.58	11.70	2.12
17	[4.4.2]propella-11,12-dione[h]	8.65	10.4	1.75
18	[4.4.2]propella-3-ene-11,12-dione[h]	8.60	10.5	1.9
19	[4.4.2]propella-3,8-diene-11,12-dione[h]	8.70	~10.7	~2.0
20	3,3,7,7-tetramethyl-1,2-cycloheptanedione	8.70	10.60	1.90
21	3,3,7,7-tetramethyl-5-oxa-1,2-cycloheptanedione	8.90	10.90	2.0
22	3,3,7,7-tetramethyl-7-thia-1,2-cycloheptanedione	8.75	10.65	1.90
23	3,3-dimethylindandione[i]	8.7	10.8	2.1
24	diphenylglyoxal[i]	9.1	11.1	2.0
25	camphorquinone[i] (3,7,7-trimethylbicyclo[2.2.1]hept-2,3-dione)	8.71	10.46	1.75
26	bicyclo[2.2.1]hept-2,3-dione[j]	9.00	10.85	1.85
27	7,7-cyclopropylbicyclo[2.2.1]hept-2,3-dione[j]	8.75	~10.7	~1.95
28	tetrafluoro-1,2-cyclobutanedione[g]	10.45	13.04	2.59
29	7-oxabicyclo[2.2.1]heptane-2,3-dione[f]	9.2	11.5	2.3
30	bicyclo[2.2.1]hept-5-ene-2,3-dione[j]	8.73	11.17	2.44
31	5-methylbicyclo[2.2.1]hept-5-ene-2,3-dione[j]	8.50	10.90	2.40
32	7,7-dimethylbicyclo[2.2.1]hept-5-ene-2,3-dione[j]	8.50	10.80	2.30
33	7,7-cyclopentylbicyclo[2.2.1]hept-5-ene-2,3-dione[j]	8.45	10.75	2.30
34	7,7-cyclopropylbicyclo[2.2.1]hept-5-ene-2,3-dione[j]	8.50	~10.95	~2.45
35	7-isopropenylbicyclo[2.2.1]hept-5-ene-2,3-dione[j]	8.30	10.90	2.60
36	7-oxabicyclo[2.2.1]hept-5-ene-2,3-dione[j]	8.95	11.55	2.60
37	tricyclo[3.2.2.0²,⁴]nonane-2,3-dione[f]	8.9	11.5	2.6
38	tricyclo[3.2.2.0²,⁴]non-8-ene-6,7-dione[f]	8.7	11.8	3.1
	B. β-Dicarbonyls			
1	2,2-dimethyl-1,3-propanedial[k]	10.5	9.8	0.7
2	2,4-pentanedione[k]	10.15	~9.6	~0.55
3	3-methyl-2,4-pentanedione[k]	10.05	9.43	0.62
4	3,3-dimethyl-2,4-pentanedione[k]	9.86	9.30	0.56
5	formylurea[l]	11.35	~10.6	~0.75
6	acetylurea[l]	11.1	~10.3	~0.8
7	1,3-cyclopentanedione[m]	10.40	9.53	0.87
8	2-methyl-1,3-cyclopentanedione[m]	10.18	9.40	0.78
9	2,2-dimethyl-1,3-cyclopentanedione[m]	10.05	9.34	0.71
10	succinic anhydride[n]	11.61	10.80	0.81
11	maleic anhydride[n]	11.95	11.10	0.85
12	succinimide[o]	~10.8	~10.1	~0.7
13	N-methylsuccinimide	10.71	~10.0	~0.71
14	1,3-cyclohexanedione[m]	10.04	9.60	0.44
15	2-methyl-1,3-cyclohexanedione[m]	9.81	9.48	0.33
16	2-isopropyl-1,3-cyclohexanedione[m]	9.61	9.29	0.32
17	2-tert-butyl-1,3-cyclohexanedione[m]	9.62	9.15	0.47
18	glutaric anhydride	11.17	10.58	0.59
19	glutarimide[o]	~10.5	10.05	~0.45
20	dihydrouracil[l]	11.0	~10.1	~0.9
21	uracil[l]	11.0	10.13	0.87
22	thymine[l]	10.88	10.05	0.83
23	1,3-dimethyluracil[l]	10.55	9.70	0.85
24	2,2,4,4-tetramethyl-1,3-cyclobutanedione	8.80	9.53	0.70
	C. γ-Dicarbonyls			
1	1,4-cyclohexanedione	~9.85	9.65	~0.2
2	1,4-benzoquinone[p]	10.29	9.99	0.30
3	2-methyl-1,4-benzoquinone[p,q]	10.17	9.78	0.39
4	2,5-dimethyl-1,4-benzoquinone[p]	~10.05	9.60	~0.45
5	tetramethyl-1,4-benzoquinone[p]	9.75	9.25	0.50

Table I. (*Continued*)

no. index	compd	$I(n_+)$	$I(n_-)$	Δn
6	tetrachloro-1,4-benzoquinone[p]	~10.1	9.90	~0.2
7	2,3-dichloro-5,6-dicycano-1,4-benzoquinone[p]	10.76	10.58	0.18
8	tetrafluoro-1,4-benzoquinone[p]	10.96	11.21	0.25
	D. δ-Dicarbonyls			
1	1,3-diacetylazulene[r,s]	~9.1	~9.1	~0
2	cis-bicyclo[3.3.0]octane-3,7-dione	9.78	9.45	0.33
3	4,6,8-trimethyl-1,3-diacetylazulene[s]	~8.75	~8.75	~0

[a] D. W. Turner, C. Baker, A. D. Baker, and C. R. Brundle, "Molecular Photoelectron Spectroscopy", Wiley-Interscience, New York, N.Y., 1970. [b] S. P. McGlynn and J. L. Meeks, *J. Electron Spectrosc. Relat. Phenom.*, **6**, 269 (1975). [c] J. L. Meeks, J. F. Arnett, D. B. Larson, and S. P. McGlynn, *J. Am. Chem. Soc.*, **97**, 3905 (1975). [d] J. L. Meeks and S. P. McGlynn, *Spectrosc. Lett.*, **8**, 439 (1975). [e] J. L. Meeks and S. P. McGlynn, *J. Am. Chem. Soc.*, **97**, 5079 (1975). [f] R. Gleiter, R. Bartetzko, P. Hofmann and H.-D. Scharf, *Angew. Chem., Int.Ed. Engl.*, **16**, 400 (1977). [g] E. Heilbronner, private communication. [h] D. Dougherty, J. J. Bloomfield, G. R. Newkome, J. F. Arnett, and S. P. McGlynn, *J. Phys. Chem.*, **80**, 2212 (1976). [i] J. F. Arnett, G. Newkome, W. L. Mattice, and S. P. McGlynn, *J. Am. Chem. Soc.*, **96**, 4385 (1974). [j] D. Dougherty, R. L. Blankespoor, and S. P. McGlynn, manuscript in preparation. [k] A. Schweig, H. Vermeer, and U. Weidner, *Chem. Phys. Lett.*, **26**, 229 (1974). [l] D. Dougherty, K. Wittel, J. L. Meeks, and S. P. McGlynn, *J. Am. Chem. Soc.*, **98**, 3815 (1976). [m] K. N. Houk, L. P. Davis, G. R. Newkome, R. E. Dube, and R. V. Nauman, *J. Am. Chem. Soc.*, **95**, 8364 (1973). [n] M. Almemark, J. E. Backwall, C. Moberg, B. Akermark, L. Asbrink, and B. Roos, *Tetrahedron*, **30**, 2503 (1974). [o] Enolization to the lactim form occurred to some extent with succinimide and glutarimide; the ionization values listed for these molecules, therefore, are approximate. [p] D. Dougherty and S. P. McGlynn, *J. Am. Chem. Soc.*, **99**, 3234 (1977). [q] T. Kobayashi, *J. Electron Spectrosc. Relat. Phenom.*, **7**, 349 (1975). [r] The $I(n_+)$ and $I(n_-)$ events plus an azulene $I(\pi)$ event all occur in one unresolved ionization band. The maximum of this band is 9.1 eV and the half-width is ~1 eV. [s] D. Dougherty, J. Lewis, R. V. Nauman, and S. P McGlynn, manuscript in preparation. [t] The difference Δn is defined as $\Delta n \equiv |I(n_+) - I(n_-)|$.

Table II. Mean Values of Δn and Standard Deviations (eV)

	$\overline{\Delta n}$	std dev (rms)
α-dicarbonyls[a]	1.9	0.15
β-dicarbonyls[b]	0.65	0.17
γ-dicarbonyls[c]	0.3	0.13
δ-dicarbonyls	(0.1)	

[a] Only the first 27 entries in Table IA were used to calculate $\overline{\Delta n}$; The Δn values for the last 11 entries are modified by anomalous interactions peculiar to these molecules (see text). [b] All entries in Table IB, TMCBD included, were used. It should be noted that the MO order in TMCBD is the reverse of that for the other β-dicarbonyls. [c] All entries in Table IC, including tetrafluoro-1,4-benzoquinone, were used. It should be noted that the MO order in this last molecule is the reverse of that for the other γ-dicarbonyls.

smaller. The larger values of Δn for the uracils (**20–23**, Table IB) are probably due to the nonsymmetrical environments of the individual carbonyl units.

The $I(n)$ events of 1,3-cyclopentanedione and 1,3-cyclohexanedione are shown in Figure 4. The Gaussian and blue-degraded band shapes are very evident for 1,3-cyclopentanedione, but are less clear for 1,3-cyclohexanedione. The $I(n_+^0)$ band in the latter molecule is partially obscured by overlap with $I(n_-^\sigma)$, but there is little doubt that the $I(n_+^0)$ event is the sharper. The $I(n)$ band shapes of all noncoaxial β-dicarbonyls exhibit this pattern: the Gaussian band occurs at lower ionization energies than the blue-degraded band.

The vibrational structure associated with the n_+^0/n_-^σ ionization events, when observed, appears to follow the same σ/0 categorization found for the α-dicarbonyls. The $I(n_+^0)$ bands of entries **20–23** of Table Ib all exhibit a progression in ~1500 cm^{-1}, presumably a carbonyl stretch, and the vertical and adiabatic events coincide. The $I(n_-^\sigma)$ events of entries **21** and **22** of Table IB, on the other hand, exhibit progressions in 1250 and 1300 cm^{-1}, respectively, and the vertical transitions occur at the second member of a weakly defined progression of three members.

The observed $I(n)$ band shapes of the noncoaxial β-dicarbonyls may be rationalized using the MOs of Figure 3. Since $I(n_-^\sigma) < I(n_+^0)$, it follows that the n_-^σ MO must be more skeletally involved than n_+^0. This conclusion also follows from
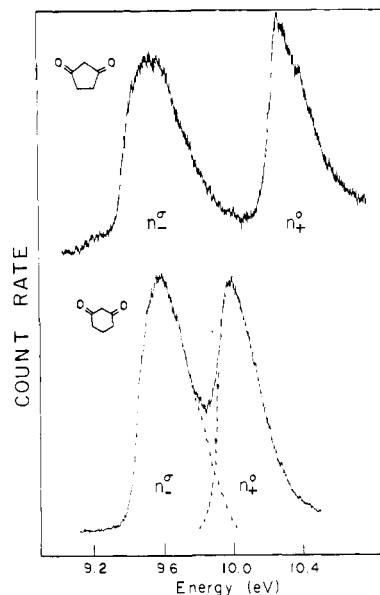

Figure 4. The He I photoelectron bands $I(n_-^\sigma)$ and $I(n_+^0)$ of 1,3-cyclopentanedione and 1,3-cyclohexanedione.

Figure 3. The directed carbon–carbon bonds of n_-^σ contribute significantly to bonding between the carbonyls and, therefore, ejection of an electron from n_-^σ should produce a geometry change in the σ structure between the carbonyls and generate a Gaussian UPS band. In n_+^0, the bonds between the carbonyls are not directed; in fact, the atomic orbital on carbon 2 (C_2) is effectively nonbonding (i.e., there is little overlap with the AOs on C_1 and C_3). Ejection of an electron from n_+^0, therefore, should produce a negligible effect on the skeletal geometry, causing $I(n_+^0)$ to be blue-degraded.

2,2,4,4-Tetramethyl-1,3-cyclobutanedione (TMCBD). TMCBD is unique among β-carbonyls in that the MO order[1] is $n_+^0 > n_-^\sigma$. The UPS of TMCBD is shown in Figure 5. The inversion, relative to other β-dicarbonyls, of blue-degraded and Gaussian shapes is striking. Since TMCBD is the only β-dicarbonyl with coaxial carbonyl groups and the only one in which the UPS band shapes are inverted, we consider TMCBD separately.
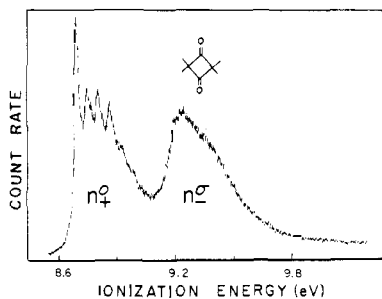
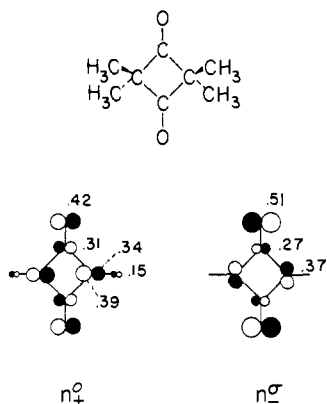**Figure 5.** The low-energy He I photoelectron spectrum of 2,2,4,4-tetramethyl-1,3-cyclobutanedione (TMCBD).

Figure 6. MO diagrams (CNDO/s) for n_+^0 and n_-^σ of 2,2,4,4-tetramethyl-1,3-cyclobutanedione. Geometrical parameters are taken from the crystallographic data of ref 26a, with the exception of the C–CH₃ bond lengths which are taken from the electron diffraction data of ref 26b.

The n MOs of TMCBD are shown in Figure 6. The n_+/n_- functions mix unequally with the skeletal σ orbitals. The n_+ MO contains an admixture of one of the degenerate pair of HOMOs of the cyclobutane moiety, while the n_- MO contains an admixture of the deeper b_1 MO of the parental four-membered ring. Since the O=C–C angle in TMCBD (135°) is larger than that of other β-dicarbonyls (~120°), the overlap of the carbonyl group orbitals with the skeletal σ orbitals is smaller for TMCBD than for noncoaxial β-dicarbonyls. Consequently, we believe that it is item (2) of the interaction model, namely, energy denominator effects, and not item (3), namely, overlap effects, which dominates the relative energetics of the n_+/n_- MOs. Thus, we expect n_+ to be less tightly bound than n_-.

By the same token, n_+ contains more ring skeletal character than n_-. However, the ring group orbital in n_+ possesses three nodes whereas that in n_- possesses only two nodes. Consequently, despite its greater component of ring σ character, the n_+ MO is less bonding skeletally than n_- because of the poor skeletal binding characteristics of the n_+ ring complement. This conclusion also follows from inspection of the MOs of Figure 6. The net result is that the ionization energies lie in the order

$$I(n_+) < I(n_-)$$

and that the relative ring σ characteristics merit the labeling n_+^0 and n_-^σ in accord with the observed vibrational structure of the two UPS bands.

In Figure 6, as in Figure 3, the Gaussian band shape corresponds to the MO with directed-bond σ orbitals. It is suggested, therefore that the Gaussian and blue-degraded band shapes are as dependent on the form of the admixed ring group orbital as they are on the degree of n/σ mixing.

γ-Dicarbonyls. The data set of γ-dicarbonyls is small. Ad-
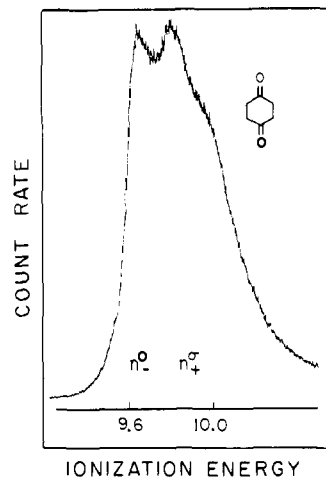

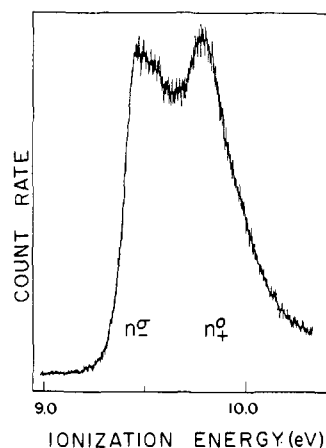**Figure 7.** The low-energy He I photoelectron spectrum of 1,4-cyclohexanedione.

Figure 8. The low-energy He I photoelectron spectrum of cis-bicyclo[3.3.0]octane-3,7-dione.

equately resolved UPS data are available only for eight molecules. These data are listed in Table IC, and Δn is plotted in Figure 2. Furthermore, the carbonyl groups are coaxial in all eight molecules. As for β-dicarbonyls, coaxial carbonyl groups should exhibit an n MO order which is inverted relative to that for noncoaxial γ-dicarbonyls.

The predicted MO order in noncoaxial γ-dicarbonyls is $n_+ > n_-$, according to CNDO/s calculations for 1,4-butanedial in various conformations. The calculated values of Δn are ~0.2 eV. Bonding considerations suggest the further labeling n_+^σ and n_-^0. This latter labeling is based on the fact that the σ MO which mixes with n_+ is of a directed bond nature whereas the σ MO which mixes with n_- possesses negligible bonding between carbons 2 and 3 (i.e., the central bond). Unfortunately, no UPS data being available, computations provide the only data access for noncoaxial γ-dicarbonyls.

The six-membered ring is the smallest cyclic configuration that can accommodate γ-dicarbonyl units as an integral part of the ring. The 1,4-benzoquinones are the most important examples of this type.[1,2,17,19,20,23,25] The low-energy UPS of 1,4-cyclohexanedione is shown in Figure 7. This molecule may exist in three conformations (symmetries): boat (C_{2v}), chair (C_{2h}), and skew (D_2). The skew conformation in which the carbonyl groups are coaxial is preferred.[1] Consequently, the spectrum of Figure 7 consists of an average over all three conformations, the skew being dominant.

Any two lone-pair orbitals separated by an odd number of bonds should exhibit[23] the MO order $n_+ > n_-$. This conclusion follows from the unique location of the central σ bond and the

DICARBONYL COMPOUNDS
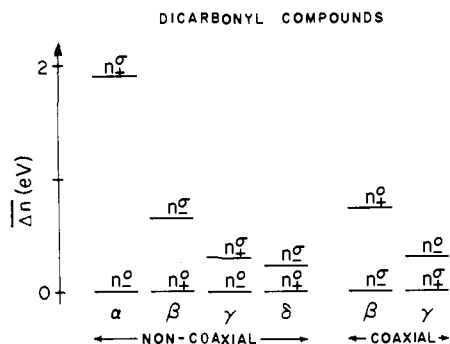

Figure 9. A summary of results for the nonbonding MOs of dicarbonyls. The various dicarbonyls are categorized by their carbonyl group separations (α, β, etc.) and divided into two classes (coaxial and noncoaxial). Values of Δn are taken from Table II. The separation Δn shown for δ-dicarbonyls is, for convenience, enlarged by a factor of 2.

coupling which it mediates. This coupling destabilizes n_+ in the same way as in the α-dicarbonyls. In 1,4-benzoquinone, however, this σ orbital extends around the six-membered ring in a very strongly bonding manner.[17] Thus, the energy denominator criterion suggests that very little n_+/σ mixing will occur. Conversely, the ring σ orbital that mixes with n_- has a node through the center of the ring and perpendicular to the line of the carbonyls. This ring σ orbital, therefore, is of much higher energy than the one which interacts with n_+. By the energy denominator criterion, then, n_- should be destabilized to a greater extent than n_+. Thus, the expected MO order[17,19] in the 1,4-benzoquinones is $n_-{}^0 > n_+{}^\sigma$. The observed blue-degraded and Gaussian band shapes are quite distinct and in agreement with these conclusions. The coaxial arrangement of the carbonyl groups in the 1,4-benzoquinones produces an inversion of the $n_+{}^\sigma > n_-{}^0$ MO order expected for noncoaxial γ-dicarbonyls.

An exception occurs in tetrafluoro-1,4-benzoquinone,[17] where $n_+{}^\sigma > n_-{}^0$. It is of interest that electron-donating methyl groups increase Δn in the benzoquinones, while electron-withdrawing groups decrease Δn, and that, in the perfluoro derivative, the expected MO order undergoes inversion.

δ-**Dicarbonyls.** CNDO/s calculations on 1,5-pentanedial yield $n_-{}^\sigma > n_+{}^0$, just as in noncoaxial β-dicarbonyls. Computed Δn values for several molecular conformations are effectively constant at $\sim$0.4 eV.

The UPS data for three δ-dicarbonyls are listed in Table ID and the Δn values are plotted in Figure 2. Since only three compounds are listed, the results are hardly general. However, in view of the nature of these molecules, it is not likely that this list will be appreciably lengthened.

The UPS of compound 2 of Table ID is shown in Figure 8. The ionization bands are not well resolved; nonetheless, the band at higher ionization energy does appear to be sharper, in accord with its expected $n_+{}^0$ nature.

Conclusions

The conclusions of this work follow from Table I and Figure 2 and are summarized in Figure 9.

The magnitude of the through-bond interaction, as measured by Δn, decreases rapidly with increasing carbonyl sep-

aration. The concept of an average interaction energy, gauged by Δn, is valid.

The energetic order of the nonbonding MOs can be synopsized by dividing the carbonyls into two classes: those in which the carbonyl groups are coaxial, and those in which they are not. Figure 9 is a schematic of the results. The only exceptional case is tetrafluoro-1,4-benzoquinone.

The UPS band shape differences are qualitatively rationalized. The form of the skeletal σ MOs determines band shape characteristics. The Gaussian band is always associable with the n MO which contains directed σ skeletal components, while the blue-degraded band is always associable with the n MO in which the skeletal σ orbital is effectively nonbonding across the central bond between the carbonyls. As shown in Figure 9, the Gaussian shaped UPS band occurs at lower ionization energy in the noncoaxial dicarbonyls and the blue-degraded band occurs at lower ionization energy in the coaxial dicarbonyls.

References and Notes

(1) D. O. Cowan, R. Gleiter, J. A. Hashmall, E. Heilbronner, and V. Hornung, *Angew. Chem., Int. Ed. Engl.*, **10**, 401 (1971).
(2) J. R. Swenson and R. Hoffmann, *Helv. Chim. Acta*, **53**, 2331 (1970).
(3) R. Hoffmann, *Acc. Chem. Res.*, **4**, 1 (1970).
(4) T. K. Ha and W. Hug, *Helv. Chim. Acta*, **54**, 2278 (1971).
(5) K. N. Houk, L. P. Davis, G. R. Newkome, R. E. Duke, and R. V. Nauman, *J. Am. Chem. Soc.*, **95**, 8364 (1973).
(6) A. Schweig, H. Vermeer, and U. Weidner, *Chem. Phys. Lett.*, **26**, 229 (1974).
(7) M. Almemark, J. E. Bäckvall, C. Moberg, B. Åkermark, L. Åsbrink, and B. Roos, *Tetrahedron*, **30**, 2503 (1974).
(8) J. L. Meeks, J. F. Arnett, D. Larson, and S. P. McGlynn, *Chem. Phys. Lett.*, **30**, 190 (1975).
(9) S. P. McGlynn and J. L. Meeks, *J. Electron Spectrosc. Relat. Phenom.*, **6**, 269 (1975).
(10) J. L. Meeks, J. F. Arnett, D. Larson, and S. P. McGlynn, *J. Am. Chem. Soc.*, **97**, 3905 (1975).
(11) S. P. McGlynn and J. L. Meeks, *J. Electron Spectrosc. Relat. Phenom.*, **8**, 85 (1976).
(12) J. L. Meeks, H. J. Maria, P. Brint, and S. P. McGlynn, *Chem. Rev.*, **75**, 603 (1975).
(13) J. L. Meeks and S. P. McGlynn, *Spectrosc. Lett.*, **8**, 439 (1975).
(14) J. L. Meeks and S. P. McGlynn, *J. Am. Chem. Soc.*, **97**, 5079 (1975).
(15) D. Dougherty, K. Wittel, J. Meeks, and S. P. McGlynn, *J. Am. Chem. Soc.*, **98**, 3815 (1976).
(16) D. Dougherty, J. J. Bloomfield, G. R. Newkome, J. F. Arnett, and S. P. McGlynn, *J. Phys. Chem.*, **80**, 2212 (1976).
(17) D. Dougherty and S. P. McGlynn, *J. Am. Chem. Soc.*, **99**, 3234 (1977).
(18) R. Gleiter, R. Bartetzko, P. Hofmann, and H.-D. Scharf, *Angew. Chem., Int. Ed. Engl.*, **16**, 400 (1977).
(19) G. Lauer, W. Schäfer, and A. Schweig, *Chem. Phys. Lett.*, **33**, 312 (1975).
(20) T. Kobayashi, *J. Electron Spectrosc. Relat. Phenom.*, **7**, 349 (1975).
(21) D. Dougherty, R. L. Blankespoor, and S. P. McGlynn, manuscript in preparation.
(22) T. Koopmans, *Physica (Utrecht)*, **1**, 104 (1934); K. Wittel and S. P. McGlynn, *Chem. Rev.*, **77**, 745 (1977).
(23) R. Hoffmann, A. Iwamura, and W. J. Hehre, *J. Am. Chem. Soc.*, **90**, 1499 (1968).
(24) C. R. Brundle, M. B. Robin, and N. A. Kuebler, *J. Am. Chem. Soc.*, **94**, 1466 (1972).
(25) D. W. Turner, C. Baker, A. D. Baker, and C. R. Brundle, "Molecular Photoelectron Spectroscopy", Wiley-Interscience, New York, N.Y., 1970.
(26) (a) C. D. Shirrell and D. E. Williams, *Acta Crystallogr., Sect. B*, **30**, 245 (1974); (b) W. N. Lipscomb and V. Shomaker, *J. Chem. Phys.*, **14**, 475 (1946).